Mediterranean Marine Science

Vol 15, No 4 (2014)

Vol 15, No 4 (2014) special issue

The influence of the Guadalquivir river on spatio-temporal variability in the pelagic ecosystem of the eastern Gulf of Cádiz

I. CABALLERO, E. P. MORRIS, L. PIETRO, G. NAVARRO

doi: 10.12681/mms.844

Research Article

Mediterranean Marine Science
Indexed in WoS (Web of Science, ISI Thomson) and SCOPUS
The journal is available on line at http://www.medit-mar-sc.net
DOI: http://dx.doi.org/10.12681/mms844

The influence of the Guadalquivir River on the spatio-temporal variability of suspended solids and chlorophyll in the Eastern Gulf of Cadiz

I. CABALLERO, E.P. MORRIS, L. PRIETO and G. NAVARRO

Department of Ecology and Coastal Management, Instituto de Ciencias Marinas de Andalucia (ICMAN-CSIC), Puerto Real, 11510, Cadiz

Corresponding author: isabel.caballero@icman.csic.es

Handling Editor: Ioanna Siokou

Received: 21 March 2014; Accepted: 21 October 2014; Published on line: 22 December 2014

Abstract

This study examines the spatio-temporal variability of the turbidity plume and phytoplankton biomass (in terms of chlorophyll) in the marine region influenced by the Guadalquivir estuary using ocean colour images over a period of 11 years (2003-2013). The area of the turbidity plume was calculated using water-leaving radiance at 555 nm (*nLw555*). Climatologic and monthly averages showed recurrent high *nLw555* levels in winter and high chlorophyll in spring. Similar variability was confirmed by Empirical Orthogonal Function (EOF) analysis of 8-day composite images, illustrating the existence of different regions with similar behaviour. The first EOF mode explained 60.7% and 31% of the variability in *nLw555* and chlorophyll, respectively, and was associated with enhanced Total Suspended Solids (*TSS*) in autumn-winter and phytoplankton blooms in winter-spring periods. The results confirmed that the development of the turbidity plume and subsequent phytoplankton blooms were strongly regulated by river discharges and precipitation. Indeed, inter-annual variation in *nLw555* was consistent with changes in the large-scale climate index, the North Atlantic Oscillation, a proxy for regional rainfall patterns. In the case of phytoplankton biomass, the second EOF mode revealed differentiation between offshore and near shore areas, the latter characterized by delayed development of phytoplankton blooms due to light limitation by high *TSS*. This suggests that the stability of the water column, via its influence on phytoplankton light-limitation, also influenced the timing and magnitude of phytoplankton bloom events. The dynamics of the Guadalquivir estuary turbidity plume is a crucial factor for the pelagic ecosystem of the Eastern Gulf of Cadiz, governing phytoplankton productivity.

Keywords: Water quality, remote-sensing, MODIS, EOF analysis, Gulf of Cadiz, Guadalquivir estuary.

Introduction

The Guadalquivir river is one of the largest rivers in Spain with a total length of 680 km and a drainage basin of 63822 km^2 (Granado-Lorencio, 1991). Located on the South-western coast of the Iberian Peninsula, the last 110 km of the river is the Guadalquivir estuary (Fig. 1), with a width of 800 m near its mouth, 150 m at the head, and a mean depth of 7.1 m. The estuary is a well-mixed mesotidal system with a longitudinal salinity gradient (Vanney, 1970), a semidiurnal tidal period and maximum tidal range of 3.5 m during spring tides (Díez-Minguito *et al.,* 2012). Tidal influence extends up the Guadalquivir as far as the Alcala del Rio dam, 110 km upstream from the river mouth at Sanlucar de Barrameda (Fig. 1). The original transport of material from the river basin has been drastically diminished by the construction of numerous reservoirs (the actual number of dams is 55). Annual discharges from Alcala del Rio dam have been strongly altered since the 1970s, in conjunction with the development of intensive agriculture and increased water demands. Terrestrial contributions to the estuary have decreased by about 60%, from 158.55 m^3/s (1931–1981) to 63.42 m^3/s (1981–2000) (Navarro *et al*., 2012b). Discharges from Alcala del Rio dam represent approximately 80% of the estuary's freshwater supply. The substantial fluvial inputs associated with the discharge of Guadalquivir and also major rivers such as Guadalete, Guadiana and Tinto-Odiel are the main supply of the continental shelf of the Gulf of Cádiz (about 50 km wide from the East of Cape Santa Maria to the West of the Bay of Cadiz). The outer estuary and its coastal fringe are characterized by large loads of suspended matter resulting in high turbidity levels (Navarro *et al.,* 2012b) and high biological productivity (Navarro & Ruiz, 2006; Prieto *et al.*, 2009). This estuarine environment is ecologically and socio-economically important, resulting in high levels of pressure from numerous stakeholders (Bhat & Blomquist, 2004; Ruiz *et al.,* 2014). In addition, the Gulf of Cadiz region is characterized by strong seasonality and important synoptic weather events (Prieto *et al.,* 2009), which largely control chlorophyll concentrations and suspended material. Hence, there is a need for comprehensive studies on

the natural functioning of the region so as to allow assessment of the potential consequences of anthropogenic actions. Enhancing knowledge about the factors influencing plume and bloom dynamics is important for coastal decision-makers, who are responsible for the challenging short-term management and long-term policy decisions to protect water quality and human health.

Estuarine plumes in coastal regions are significantly influenced by land-derived discharge emanating from an estuary (Morris *et al.,*1995). As a result, the turbidity plume may be biogeochemically characterized by the significantly inorganic nutrients and dissolved trace heavy metal enrichment compared with offshore waters (Mendiguchía *et al.,* 2007). At the same time, sediment load and other substances from the rivers diminish light transmittance in the sea. Chemical transport and biogeochemical interactions within these areas may be key factors in several important processes, including phytoplankton production, eutrophication and global geochemical cycling. Estuarine plume region is usually located in the lower reaches of an estuary, where conditions are favourable for phytoplankton growth, resulting in enhanced biological activity. As a consequence, chlorophyll blooms in estuarine plumes (impacting adjacent coastal areas) can be potentially higher than in nearby ocean regions (Pennock, 1985). However, in turbid environments, light availability plays a fundamental role as the energy source for phytoplankton growth (Cloern, 1987), and it also influences phytoplankton community structure and algal competition (Reynolds, 1998).

Furthermore, water clarity or transparency is important for the functioning of estuarine and coastal ecosystems; directly influencing primary productivity and acting as an indicator of nutrient loading and sediment dynamics (Ruiz *et al.,* 2013). Three main types of material are responsible for the colour and transparency of the water: phytoplankton and suspended particles related to algal activity, non-algal suspended solids (Total Suspended Solids, *TSS*), and humic substances (Coloured Dissolved Organic Matter, *CDOM*). Sources of *TSS* include terrestrial inputs from river basins and anthropogenic discharges, such as industrial or urban effluents, fringing estuarine habitats, such as salt marshes, and resuspension of sediments. Often, these inputs are enriched with organic matter and nutrients (organic and inorganic), and depending on their source, may include potentially toxic compounds, such as heavy metals and pharmaceuticals (González-Mazo *et al.,*1998; Kidd *et al.,* 2007; Mendiguchía *et al.,* 2007). Hence, tracing the dynamics of river-estuary plumes within coastal zones can also assist in understanding the effects of a range of other potential stressors.

Integrated management of transitional and coastal waters is a priority, e.g. to comply with the EU water framework directive (WFD); however cost-effective methods to monitor water quality at large synoptic scales are lacking. Tools that can provide recurrent, widespread, and consistent observations, allowing the detection of changes in water conditions are sorely needed. Frequent synoptic information on suspended matter and chlorophyll is difficult to obtain using in situ monitoring networks, since the spatial distribution of suspended matter (such as chlorophyll) is highly heterogeneous. Furthermore, standard monitoring programs can be costly and time-consuming. As a consequence, sparse spatial and temporal data resolution is obtained, without guaranteeing a representative coverage of the variability in complex heterogeneous environments such as coastal waters and estuaries. During the past two decades, there have been significant advances in the development of satellite-borne sensors that can provide synoptic views of environmental parameters in coastal zones. Ocean colour remote sensing is now recognized as a suitable and cost-effective technique for the large-scale control of coastal water quality, based on optically active water characteristics. The collection and interpretation of earth observation imagery from optical sensors provides a unique set of capabilities for monitoring the state and trend of the environment, with great potential to overcome some of the spatial and temporal uncertainties inherent in in-situ measurements. However, satellite platforms also have limitations with respect to adequate spatial resolution, correct sensitivity, sensor calibration and image processing software; such limitations become more apparent when the data obtained are applied to specific coastal environments. Other limiting factors are atmospheric correction and bio-optical algorithms, since they are generally devised to convert ocean observations to consistent and accurately retrieved water-quality parameters only in specific regions (Sathyendranath, 2000; Miller *et al.,* 2005). The ocean colour of the Guadalquivir estuary is affected by a variety of processes typical of environments with Case-II waters (i.e. the optical properties do not co-vary with chlorophyll content), including phytoplankton blooms, sediment plumes, and other episodic phenomena, such as runoff events (Morel *et al.,* 2006).

The aim of the present study is to use Moderate Resolution Imaging Spectroradiometer (MODIS) imagery to derive water-quality parameters (Total Suspended Solids and chlorophyll) related to phytoplankton dynamics and the pelagic ecosystem in the coastal zone adjacent to the Guadalquivir estuary. The work is motivated by the need to understand and predict the phenomena that control the exchange of riverine-estuarine material with the coastal region. Results of the validation of remotely-sensed observations and in situ measurements are presented, allowing the evaluation of the effectiveness of the MODIS sensor for monitoring key water quality parameters in the vicinity of a large highly turbid estuary. We then investigate the turbidity plume and phytoplankton bloom dynamics using more than 11 years of high temporal resolution satellite observations. Finally, by matching the major modes of spatio-temporal variability derived from

the images with meteorological and oceanographic data sources, we provide indications as to how local climatology and physical oceanography modulate the role of the Guadalquivir river in the regional pelagic ecosystem of the Eastern Gulf of Cadiz.

Materials and Methods

Satellite Imagery

Satellite ocean colour images were obtained from the MODIS sensor on the Aqua multispectral platform. This sensor provided daily or better coverage of the Gulf of Cadiz study area, although clear-sky images were obtained for about half of the days during the period of interest. All available images of chlorophyll concentration ([*Chl*], mg/m^3), Remote Sensing Reflectance of the 555 nm wavelength band (*Rrs555*, sr^{-1}), diffuse attenuation coefficient for downward irradiance at 490 nm wavelength (Kd_{490}, m^{-1}), and the Photosynthetically-Active Radiation (PAR, Einstein / m^2 / day) at medium spatial resolution (1 km), covering the region of interest and spanning the years from 2003 to 2013, were ordered and downloaded via-ftp from the Ocean Color Website (http://oceancolor.gsfc.nasa.gov). The MODIS algorithm to retrieve [*Chl*] corresponds to OC3M (O'Reilly *et al*., 2000).

SeaDAS image analysis software (SeaWiFS Data Analysis System, version 6. (http://seadas.gsfc.nasa.gov) was used to read and remap the data to a Mercator projection at 1 km resolution. Upon downloading MODIS data to a local system, the data were displayed to assess image quality. During data processing, checks are made for different defined conditions. We used the standard SeaDAS algorithm with the ''LAND'' and ''CLOUD'' flags to remove the data unintentionally interpolated among others applied as masks with L2_flags, indicating whether any algorithm failure or warning conditions occurred for any pixel. These additional and relevant quality control tests were used to discard all suspicious and low-quality data points, thus ensuring that only the most reliable data were retained for analysis (see Table 1 for specific information). They correspond to the flags masked during Level 3-ocean colour processing.

These generated data files were edited and analyzed using MATLAB 7.10.0 - R2010a (c) software, and the study area was then subset from the images to a Region Of Interest (ROI) with geographic coordinates 36.25º N - 37.25º N, 7.5º W - 6.1º W (Fig. 1). *Rrs555* images were converted to the normalized water-leaving radiance (*nLw555*, mW/cm^2 µm sr, normalized to a zenith viewing geometry at the mean Earth-Sun distance) as *nLw555* = F_0 x *Rrs555*, where F_0 is the annual spectral mean extraterrestrial solar irradiance, also called the solar constant. For the Aqua 545-565 nm band, the F_0 value corresponds to 186.09 mW/cm^2 µm (Neckel, 1984).

In this work, the river plume was operationally defined as a water mass with optical properties clearly different from those of the water masses in the vicinity of the estuary mouth. For this backscattering resulting in high values of upwelling radiation in the green-yellow band (λ = 555 nm) was used. The *nLw555* product is commonly utilized to distinguish river plumes, and was strongly correlated with *TSS* concentration ([*TSS*]) in near-surface waters (Lahet *et al.,* 2001; Loisel *et al.,* 2001; Toole & Siegel, 2001; Otero & Siegel, 2004; Nezlin & Di Giacomo, 2005; Nezlin *et al.,* 2005; Thomas & Weatherbee, 2006). For each scene, the plume extension was delimited by thresholding of the *nLw555* image. The threshold between "plume boundary" and coastal waters was defined as 1.3 mW/cm^2 µm sr (Otero & Siegel, 2004; Nezlin & DiGiacomo, 2005; Nezlin *et al.,* 2005; Valente & da Silva, 2009). Visual examination of a subset of images suggested that this value adequately defined the river plume (data not shown). Hence, this work has focused on the plume areas using indicator *nLw555* values as a proxy of [*TSS*]. Quantitative estimation of the plume extent was made by counting the number of pixels with *nLw555* values >1.3 mW/cm^2 µm sr and multiplying by the pixel size (1 km^2).

The diffuse attenuation coefficient for photosynthetically active radiation (Kd_{PAR}) can be routinely derived from present day remote sensing based on estimates of Kd_{490}. Kd_{PAR} was calculated by two relationships (Morel *et al.,* 2007; Pierson *et al.*, 2008). Kd_{PAR} was used to estimate the lower limit of the euphotic zone (defined as the depth where PAR represents 1% of surface radiation- $Z_{1\%}$) ($Z_{1\%}$=4.6 / Kd_{PAR}), following the Lambert-Beer law (Kirk, 1983). This procedure was performed for two stations (Fig. 1): nearshore station 14 (36.7133º N- 6.5100ºW, 14 km distance to coast and ~25 m depth) and offshore station 17 (36.4983º N- 6.7583ºW, 43 km distance to coast

Table 1. List of L2_flags used in the masking process to assure the quality control of the data retained for analysis. These correspond to the flags masked at Level 3-ocean colour processing.

Flag	Condition
LAND	pixel is over land
CLOUD	cloud contamination
ATMFAIL	atmospheric correction failure
HIGLINT	high sun glint
HILT	total radiance above knee
HISATZEN	large satellite zenith
CLDICE	clouds and/or ice
COCCOLITH	coccolithophores detected
HISOLZEN	large solar zenith
LOWLW	very low water-leaving radiance
CHLFAIL	chlorophyll algorithm failure
NAVWARN	questionable navigation
MAXAERITER	maximum iterations of NIR algorithm
CHLWARN	chlorophyll out of range
ATMWARN	atmospheric correction is suspect

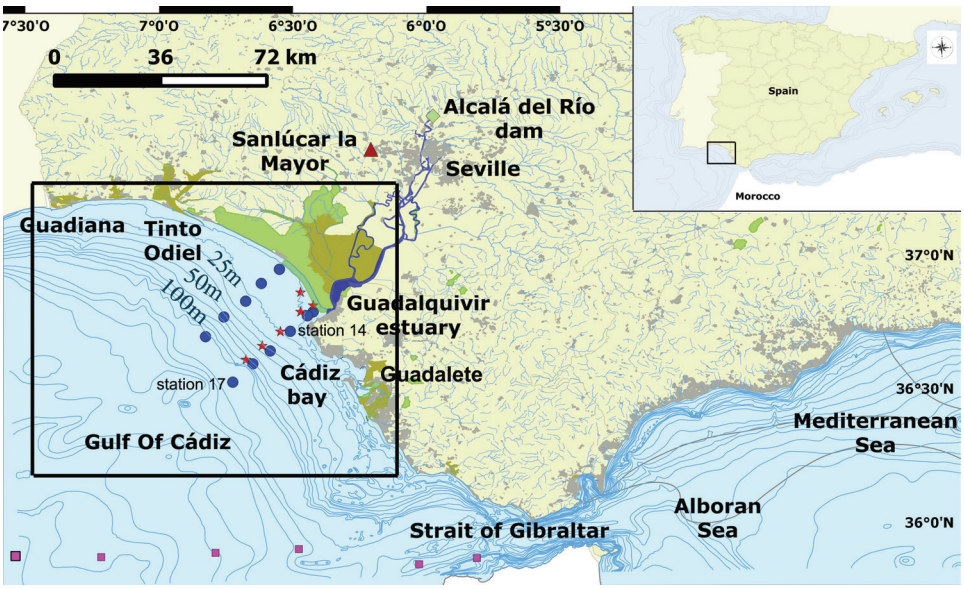

Fig. 1: a) Location of the study area (SW Iberian Peninsula). b) Map showing the Gulf of Cadiz coastal area and the Guadalquivir estuary. Blue cycles, red stars and cyan squares correspond to the stations of Fluctuaciones, Reserva and SESAME oceanographic cruises, respectively. Green diamond is Alcala del Rio dam and red triangle is Sanlucar La Mayor meteorological station. Black rectangle delimits the Region Of Interest (ROI).

and >200 m depth). *Bias* and *rmse* (root mean square error) were noticeably similar for both equations (*bias* of -0.32 m and 1.08 m and *rmse* of 0.65 m and 2.66 m, for station 14 and 17, respectively) and therefore $Z_{1\%}$ by Morel *et al*. (2007) was the only one presented.

Only images with more than 85% cloud free pixels in the ROI were used in the 11-year time series. The final products corresponded to the images ([*Chl*] and *nLw555*) after the comprehensive filtering, which are used in the validation process. Only pixels with [*Chl*] ≤ 20 mg/m^3 were considered, i.e. lower than or equal to the highest values occurring in the region (maximum value of the field campaigns). Extremely high chlorophyll values are not usually detected in the area (Sánchez-Lamadrid *et al.,* 2003; Prieto *et al.,* 2009). Daily images were further combined into 8-day and monthly means, as well as monthly climatologies and a total climatology for the 11-year period.

In-situ data

Water samples were collected near the surface (depths < 5 m) with a rosette sampler during several oceanographic field cruises in the Gulf of Cadiz (see Table 2 for detailed information). One sample for each station was collected, which were located within the first optical depth. At each sampling site, a CTD cast was performed with a Seabird Electronics Inc (Bellevue, WA, USA) CTD-SBE19plus to measure temperature, conductivity and depth. Chlorophyll analysis was performed by filtering samples through Whatman GF/F glass fiber filters (0.7 mm pore size), extracting in 90% acetone, and measuring the [*Chl*] by standard fluorometric methods (Parsons *et al.,* 1984) using a Turner Designs Model 10. The fluorometer was calibrated using pure chlorophyll from the cyanobacterium *Anacystis nidulans* (Sigma Chemical Co.) with the concentration determined spectrophotometrically. Samples to measure [*Chl*] were filtered on board and immediately deep-frozen. Pigment concentrations were subsequently determined at the ICMAN- CSIC (Marine Science Institute of Andalucia, Cadiz) laboratory within a few days of the survey. Total concentrations of suspended solids were measured gravimetrically on pre-weighted Whatman GF/F filters after rinsing with distilled water according to JGOFS protocols (UNESCO, 1994). In situ observations were chosen based on metadata indications of data quality. This selection criterion removed samples at certain situations: depth > 5m, evidence of measuring problems and defective filters. As a result, coastal [*Chl*] and [*TSS*]

Table 2. Oceanographic field cruises conducted in the Gulf of Cadiz region. Specifications of data for Total Suspended Solids (*TSS*) and chlorophyll (*Chl*) validation purposes.

Campaign	Zone	Vessel	Date	Measurements
Reserva	Coastal	RV Regina Maris	July 2002-September 2004	*TSS - Chl*
Fluctuaciones	Coastal	RV Regina Maris	May 2005-May 2007	*TSS - Chl*
SESAME I	Ocean	RV Regina Maris	April 2008	*Chl*
SESAME II	Ocean	BIO García del Cid	September 2008	*Chl*

information was selected from the "Fluctuaciones" and "Reserva" cruises. In the "SESAME" oceanic campaign, only [*Chl*] measurements were carried out. The distance between coastline and sampling stations ranged from 3 km to 35 km (average of 19 km) in the case nearshore campaigns (Reserva and Fluctuaciones) and from 10 km to 140 km in the case of the SESAME oceanic campaign. The depth at these positions varied from 15 m minimum to 150 m maximum (>1000 m in SESAME). Moreover, the Mixed Layer Depth (MLD) was estimated from the temperature and density profiles of the CTD. Several criteria have been used in the literature for the definition of MLD and a simple one is based on the changes in the properties of temperature or density with depth (Kara *et al.,* 2000). We have used the property difference in this work to define MLD for both temperature and density (difference of 0.5º and 0.125σ, respectively) since they are widely used (Kara *et al.,* 2000). In addition, MLD data have been obtained from the operational datasets routinely produced by the Global Ocean Data Assimilation System (GODAS) downloaded at http://www.esrl.noaa.gov/psd//gridded. The binary datasets corresponded to a monthly composite from 2003 to 2013. The arithmetic mean was calculated for the pixels corresponding to the study region (2º latitude x 0.6º longitude).

Daily mean discharge at the Alcala del Rio dam (Fig. 1, the main freshwater input to the Guadalquivir estuary), was obtained from the "Agencia Andaluza del Agua" (http://www.chguadalquivir.es/saih/, station code E60). Daily precipitation measured at an automatic meteorological station in Sanlucar la Mayor (Fig. 1, 37.422º N-6.254º W, station code 13) were obtained from the regional Agroclimatic Station Network (http://www.juntadeandalucia.es/agriculturaypesca/ifapa/ria).

Data on the North Atlantic Oscillation (NAO), a climatic phenomenon that greatly contributes to variability in the weather system in the North Atlantic and Europe, was provided by the Climate Analysis Section (NCAR, Boulder, USA), (http:// www.cgd.ucar.edu/cas/jhurrell/indices.html) (Hurrell, 1995). The winter (December through March) index of the NAO is based on the difference of normalized sea level pressure (SLP) between Lisbon, Portugal and Stykkishol- mur/Reykjavik, Iceland since 1864.

Validation of satellite information

To determine the quality of satellite-derived estimations of [*Chl*] and [*TSS*] in coastal waters, validation was carried out using in situ ground truth measurements acquired during several oceanographic field cruises (Table 2). The high spatio-temporal variability of estuarine water properties means that matching in situ observations with images is challenging. In this regard, different levels of spatial-temporal averaging were tested. Data match-ups were made by selecting *nLw555* and [*Chl*] values for the corresponding pixel, and also averaging the surrounding grid nodes using a 1x1 and 2x2 pixel box centred on the coordinates of the field measurements. Time differences between satellite overpasses and in situ sampling were grouped into time intervals of <1.5h, 1.5-3h, and 3-5h. These validation procedures are similar to validation works carried out by other authors (Bailey & Wang, 2001; Sá *et al*., 2008; Jamet *et al.,* 2011). Testing suggested that improved correlations between Remote Sensing (RS) and in situ-derived [*Chl*] and [*TSS*] values were observed when the shortest temporal separation window (1.5h) and smallest spatial scale (a single pixel) were used (data not shown). Hence, validation presented here only uses this limited number of higher quality match-ups. For all match-ups considered, the following statistical parameters were calculated to define the error associated with MODIS estimations; Pearson's coefficient of correlation (*r*), root mean square error (*rmse*), *bias*, maximum, and minimum values:

$$rmse = \sqrt{\frac{\Sigma(x_s - x_i)^2}{n}}$$

$$bias = \frac{\Sigma(x_s - x_i)}{n}$$

where x_i and x_s correspond to the in situ and satellite values, respectively.

An exponential adjustment was utilized in the *TSS* - *nLw555* regression because, for large [*TSS*] levels the fit is not linear. This procedure helps with possible over-

Table 3. Description of the different zones distinguished by the second and third EOF modes of normalized water leaving reflectance at 555 nm (*nLw555*) and chlorophyll (*Chl*). Further details are given in the text.

Name	Variable	Mode	Region	Spatial Coefficient
$\mathbf{Z_{2N}}$	*nLw555*	2	North	Negative
$\mathbf{Z_{2S}}$	*nLw555*	2	South	Positive
$\mathbf{Z_{3N}}$	*nLw555*	3	North	Negative
$\mathbf{Z_{3S}}$	*nLw555*	3	South	Positive
$\mathbf{A_{2C}}$	*Chl*	2	Coastal	Positive
$\mathbf{A_{2N}}$	*Chl*	2	North	Negative
$\mathbf{A_{3S}}$	*Chl*	3	South	Positive
$\mathbf{A_{3N}}$	*Chl*	3	North	Negative

correction for atmospheric effects at high [*TSS*] values, when the water reflectance contribution may no longer be negligible at larger wavelengths (Ruddick *et al*., 2000). We performed a linear regression of in situ data against MODIS [*Chl*] observations to estimate the precision of retrieval. In addition, we also compared MODIS data with the offshore cruises ("SESAME" I and II, >30km from estuary mouth) in order to characterize the quality of satellite products both in coastal waters and offshore. A previous validation exercise conducted by Navarro & Ruiz (2006) between in situ [*Chl*] measurements at 10 m (2000-2002) and Sea-viewing Wide Field-of-view Sensor (SeaWiFS) data exhibited good correlation.

Empirical Orthogonal Function (EOF) analysis

Composites of *nLw555* and [*Chl*] (8-day composite means from January 2003 to June 2013) were analyzed by decomposing their variability using the EOF (Lorenz, 1956). This methodology simplifies the dimensions of large datasets, including ocean colour images (Baldacci *et al.,* 2001; Brickley & Thomas, 2004; Xu *et al*., 2011), to a few significant orthogonal (spatially uncorrelated) modes of variability. This procedure was used to study the Gulf of Cadiz offshore region with [*Chl*] imagery from SeaWiFS imagery (Navarro & Ruiz, 2006). EOF procedures assume the data to be complete, i.e. without gaps. Therefore, previous to performing the analysis, gaps were filled by inserting the mean of the surrounding 8 pixels or 24 pixels. The final data set resulted in a total of 482 8-day composite images. The software used was MATLAB 7.10.0 with the code "*pcatool*" (Björnsson & Venegas, 1997).

EOF analysis has been extremely useful for examining ocean colour images, which have long time series and significant spatial variability, like the data sets used in this study. The importance of the EOF modes for the spatial and temporal variability was tested following the methodology by North *et al.* (1982). The interpretation of EOF modes is not always obvious, especially with difficult non-periodic signals, and should be explained with caution. Typically, the smallest modes explain much of the variance and their associated patterns are the simplest to interpret. In order to examine in detail the temporal variability of the amplitudes of each mode and identify the forcing factors, diverse oceanographic and meteorological variables have been studied and further analyzed to detect the main mechanisms of each mode. 8-day and monthly averages of the variables were contrasted with the temporal amplitudes of each mode. Statistics for each pair include the correlation determined by Pearson's coefficient of correlation (*r*) and p-value to test if the correlation is statistically significant.

Results

Validation of remotely retrieved Total Suspended Solids and Chlorophyll

One of the objectives of this study was to validate MODIS-derived water-quality parameters in the coastal region influenced by the Guadalquivir estuary. Even though a large number of in situ measurements were potentially available for the region, only 53 and 66 pairs (match-ups) for [*TSS*] and [*Chl*], respectively, were considered suitable for validation following the selection procedure and quality control of both in situ and satellite data described in Materials and Methods.

In situ [*TSS*] ranged between 28.1 and 130.4 mg/L and *nLw555* ranged between 0.1861 and 4.8011 mW/cm^2 µm sr. Both variables were highly positively correlated (Fig. 2a, $r = 0.96$, $p < 0.001$) and a non-linear predictive function for [*TSS*] (*TSS* (mg/L) =26.68*exp(0.3283**nLw555*)) gave a standard error for RS-derived [*TSS*] estimates of 5.0 mg/L. Hence, [*TSS*] appeared to be predicted with relatively good accuracy in both the offshore and nearshore regions close to the Guadalquivir estuary.

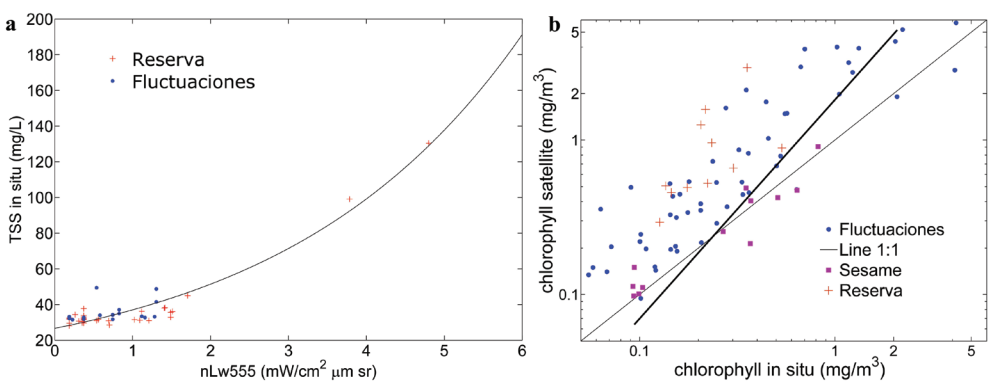

Fig. 2: a) Exponential relationship between at-sensor normalized water leaving reflectance at 555 nm *(nLw555*, mW/cm^2 µm sr) and in situ Total Suspended Solids (*TSS*, mg/L) from Fluctuaciones (dots) and Reserva (crosses) coastal campaigns. Fitted curve: *TSS* (mg/L) = 26.68*exp (0.3283**nLw555*), $n = 53$, *standard error* = 5.0 mg/L, $r = 0.96$ ($p < 0.001$). b) Scatter plot showing the comparison between in situ and at-sensor chlorophyll concentrations (*Chl*, mg/m^3) for Fluctuaciones (dots) and Reserva (crosses) coastal cruises (logarithmic axis). Regression line: $Y = 0.49 + 1.28* X$, $n = 66$, *rmse* = 1.10 mg/m^3, *bias* = 0.63 mg/m^3, $r = 0.79$ ($p < 0.001$). Squares correspond to SESAME offshore stations. The line corresponds to 1:1 ratio.

In situ and RS-derived [*Chl*] ranged from 0.055 to 4.18 mg/m^3 and 0.095 to 4.99 mg/m^3, respectively, and were positively correlated (Fig. 2b, $r = 0.79$, $p < 0.001$). Linear regression of observed and predicted values (Fig. 2b, logarithmic scale applied) revealed a *bias* of 0.63 mg/m^3 and *rmse* of 1.10 mg/m^3 (slope = 1.19). To highlight the increasing *bias* observed for nearshore to offshore RS-derived [*Chl*], a subset of 12 pairs at least 30 km offshore from the estuary mouth were also compared (Fig. 2b, "SESAME"). Whilst maximum [*Chl*] values (0.82 mg/m^3) were lower for this subset, the range of values appeared relatively comparable to nearshore values. Pairs fell close to the 1:1 line, *bias* was insignificant (*bias* ~ 0 mg/m^3) and the derived *rmse* was an order of magnitude smaller (0.086 mg/m^3).

Total Suspended Solids and Chlorophyll variability patterns

Regional satellite climatology of the Gulf of Cadiz was computed on the basis of the mean annual cycle for eleven years of MODIS data (2003-2013). Maximum *nLw555* values were located within the vicinity of the Guadalquivir and Guadalete river mouths (Fig. 3a, 4.2 and 3.9 mW/cm^2 µm sr, [*TSS*] of 103.6 and 92.2 mg/L respectively) whereas minimum values were detected offshore (0.24 mW/cm^2 µm sr, [*TSS*] = 28.7 mg/L). The typical salient pattern indicated that water clarity was usually low in the external part of the mouth, and increased offshore. The monthly climatology clearly shows the seasonal strengthening and weakening of this general pattern (Fig. 4). In winter and early spring (November-March), high values in the Guadalquivir estuary and Cadiz Bay extended along and offshore from the coastline to form a band (plume) (>1.3 mW/cm^2 µm sr). During spring and summer, ambient waters generally had low *nLw555* values with highly localized plumes restricted to the river mouth. The extent of riverine discharges during storm flood events can also be assessed using this limit, with the largest plumes found near the river mouth and further south. Extreme turbid episodes during the study

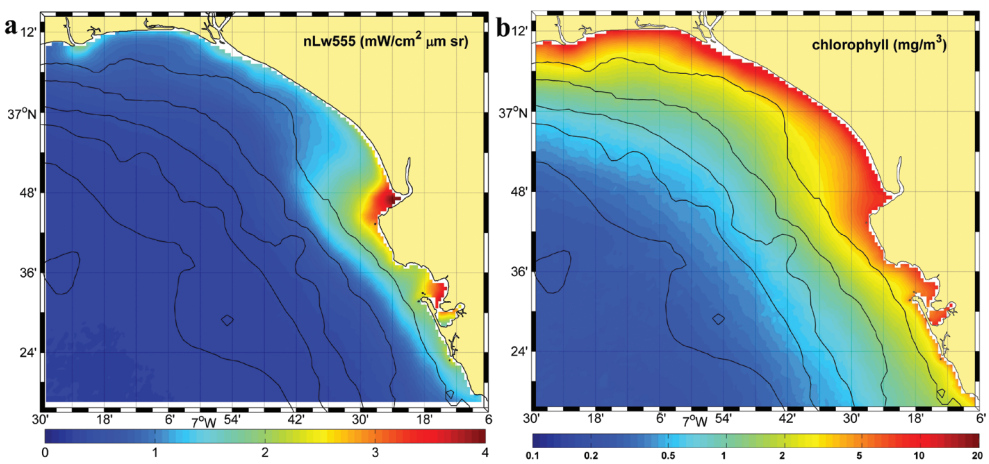

Fig. 3: Total climatology of MODIS (2003-2013): a) Normalized water leaving reflectance at 555 nm (*nLw555*, mW/cm^2 µm sr), b) Chlorophyll (*Chl*, mg/m^3). Lines represent bathymetric isolines for the Gulf of Cádiz at the intervals of 20m, 50m, 100m, 200m and 500m.

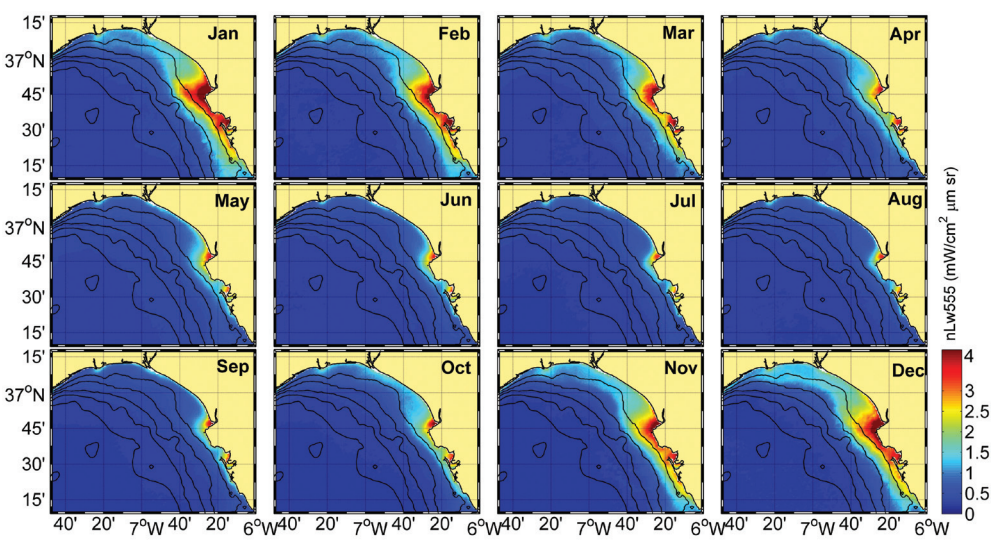

Fig. 4: Monthly climatology (2003-2013) of MODIS normalized water leaving reflectance at 555 nm (*nLw555*, mW/cm^2 µm sr). Lines represent bathymetric isolines for the Gulf of Cádiz at the intervals of 20m, 50m, 100m, 200m and 500m.

period took place during autumn and winter 2007 and throughout 2010 and 2011.

Total [*Chl*] climatology (Fig. 3b) showed that maximum concentrations (around 14 mg/m^3) were observed close to the coast (specially near the estuary), with values decreasing to a minimum of about 0.3 mg/m^3 offshore. Examining the monthly climatology (Fig. 5) revealed that higher [*Chl*] values tended to be observed in the North of the study region near the coast, especially near the Guadalquivir estuary, and lower values usually occured South of Cadiz Bay. Monthly mean [*Chl*] values peaked during March to May within the region in terms of magnitude and coverage (bloom ~40 km offshore). In addition, the offshore region presented highest [*Chl*] values (more than 0.5 mg/m^3) during March, indicating an extensive phytoplankton bloom throughout the region. During summer, offshore [*Chl*] values were low and high values were confined to shallow regions near the coast.

Modal analyses of nLw555

EOF analysis revealed three significant (North *et al.*, 1982) modes for *nLw555*, each explaining 60.7%, 6.5% and 4.7% of the variance, respectively (71.9% of the total variance, Fig. 6). Spatial coefficients of the three modes are plotted in Figure 7, where colour intensity is directly related to the amplitude of the coefficient (intensity of the phenomenon). Temporal amplitudes of the EOF modes are presented in Fig. 8.

The first *nLw555* EOF mode was positive throughout the region with the highest values occurring in a wide band extending from North of the Guadalquivir estuary to South

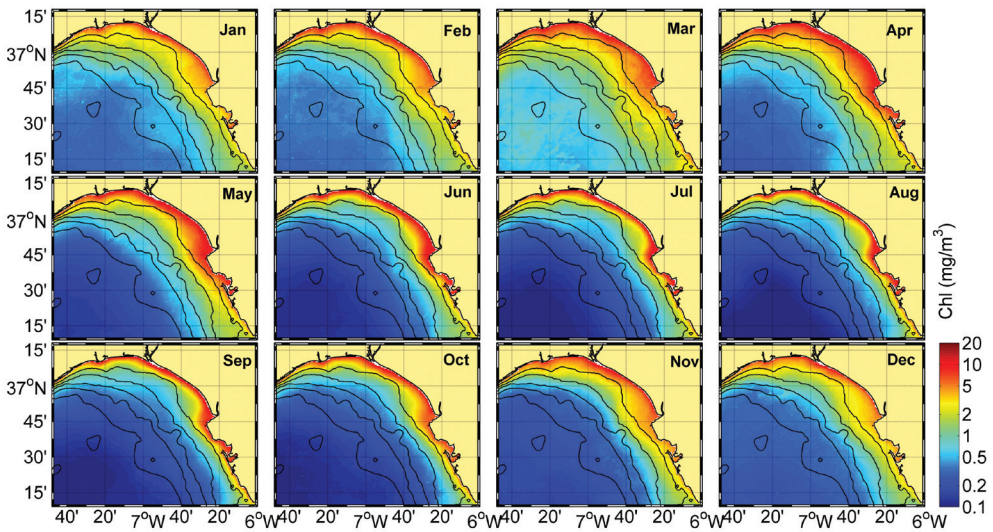

Fig. 5: Monthly climatology (2003-2013) of MODIS chlorophyll (*Chl*, mg/m^3). Lines represent bathymetric isolines for the Gulf of Cádiz at the intervals of 20m, 50m, 100m, 200m and 500m.

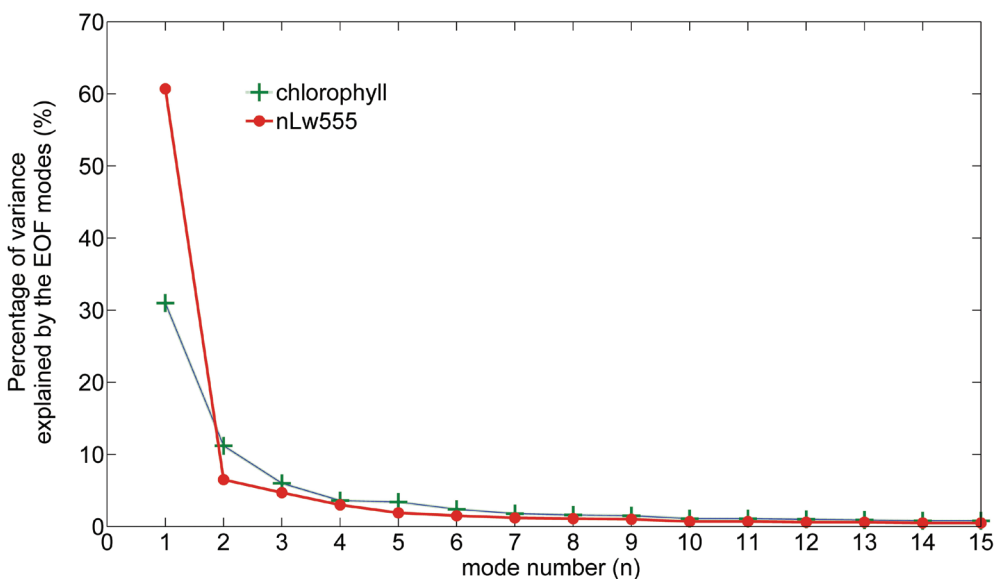

Fig. 6: Percentage of variance explained by the EOF modes for normalized water leaving reflectance at 555 nm (*nLw555*) and chlorophyll (*Chl*).

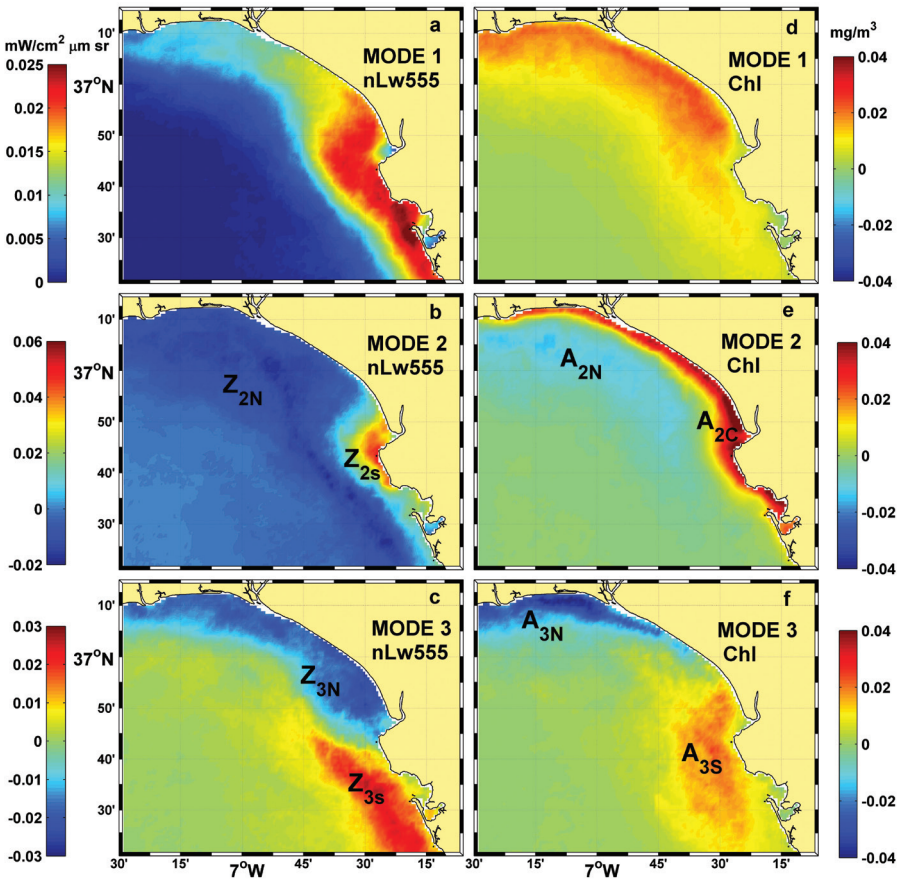

Fig. 7: Spatial coefficient maps corresponding to the a) First, b) Second, and c) Third mode from EOF analysis of normalized water leaving reflectance at 555 nm (*nLw555*, mW/cm^2 µm sr); the same for the d) First, e) Second, and f) Third mode from EOF analysis of chlorophyll (*Chl,* mg/m^3).

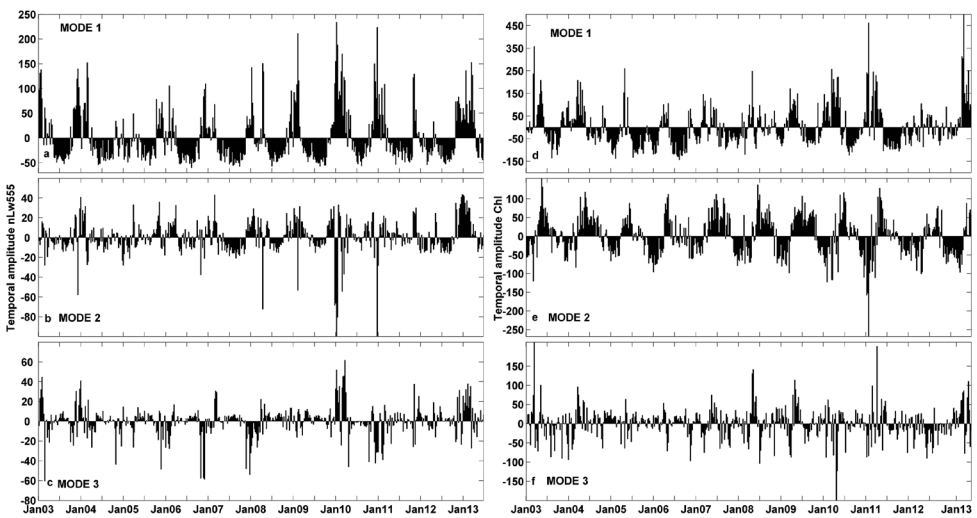

Fig. 8: Amplitude function for the a) First, b) Second, and c) Third mode from EOF analysis of normalized water leaving reflectance at 555 nm (*nLw555*); the same for the d) First, e) Second, and f) Third mode from EOF analysis of chlorophyll (*Chl*).

of Cadiz Bay (Fig. 7a). Particularly high values were found close to Cadiz bay. Spatial coefficients near zero were observed offshore, implying more stability in *nLw555* values. The amplitude function displayed seasonal oscillations between winter and summer (Fig. 8a), with positive and negative amplitudes generally in autumn-winter and spring-summer, respectively. Inter-annual variation in the magnitude of positive amplitudes was apparent, with the highest values observed in winter 2010 (January and December), whilst the magnitude of negative amplitudes was similar through the time-series. This suggests that more pronounced inter-annual variability during autumn-winter was observed closer to the coast.

The spatial pattern associated with the second *nLw555*

mode indicated two zones (Fig. 7b): The first zone (Z_{2S}) had positive coefficients that centred on the region just offshore of the Guadalquivir estuary mouth and extended further South in a confined coastal fringe. The second zone (Z_{2N}) had negative amplitudes expanding all along the coast further offshore and occupying the region north of Z_{2S}. Offshore waters had values around zero. The temporal time series of the second mode amplitude (Fig. 8b) exhibited a similar seasonal trend to the first mode, but in contrast to the first mode, included inter-annual variations in the magnitude of negative amplitudes, suggesting inter-annual variability during spring-summer in the zone north of the estuary.

The third *nLw555* mode also suggested two main spatial zones (Fig. 7c); from the northwest coast to the mouth of the river, values were negative (Z_{3N}), whereas from the limit of Z_{3N} to the most southerly area, values were positive (Z_{3S}). Whereas minimum values in Z_{3N} were observed near shore, in Z_{3S} maximum values were further offshore. The amplitude function again had a seasonal similarity to the first mode (Fig. 8c), but was more irregular. Maximum positive amplitudes were similar in magnitude to the second mode, whereas negative amplitudes were in between the other modes.

Comparison of the time-series of *nLw555* first mode amplitudes to daily rainfall (mm), daily discharges from Alcalá del Río dam (m^3/s) and the NAO index (Fig. 9), revealed that positive amplitudes, generally observed in late autumn, winter and early spring, tended to be associated with periods of high rainfall ($r = 0.47$, $p < 0.001$, Table 4), river discharges ($r = 0.50$, $p < 0.001$, Table 4) and negative NAO values ($r = -0.41$ and -0.52, $p < 0.001$, Table 4). Negative *nLw555* first mode amplitudes generally occurred in the usually drier late spring and summer months. It is noteworthy that low-medium magnitude rain-

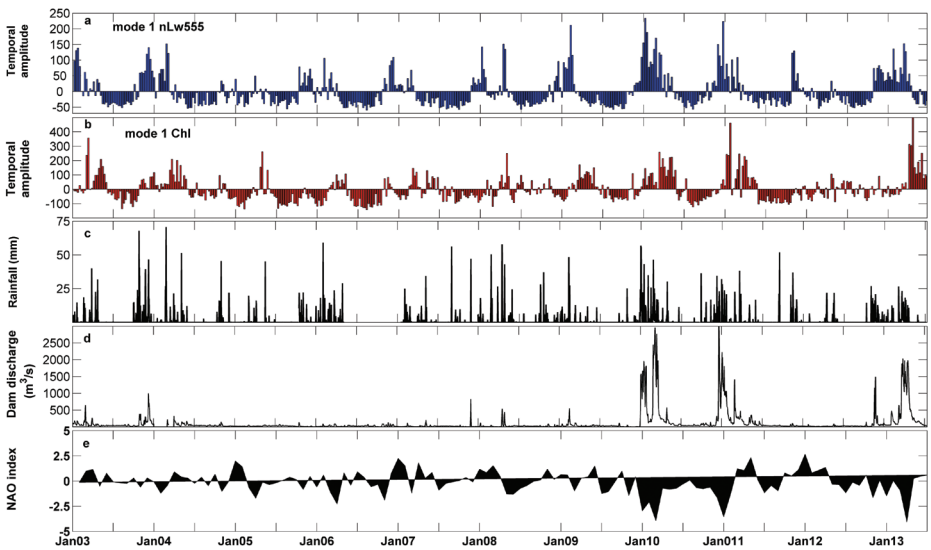

Fig. 9: Time series of: a) Temporal amplitude of EOF mode 1 for normalized water leaving reflectance at 555 nm (*nLw555*, mW/cm^2 µm sr), b) Temporal amplitude of EOF mode 1 for chlorophyll (*Chl,* mg/m^3), c) Daily precipitation average measured at the meteorological station Sanlucar La Mayor (mm), d) Daily river discharge from the Alcala del Rio dam (m^3/s), and e) Monthly time series of North Atlantic Oscillation (NAO) index.

Table 4. Pearson's correlation coefficient (r) and p-value among the temporal amplitudes of the EOF modes and precipitation from the meteorological station Sanlúcar La Mayor, discharge from Alcalá del Río dam, the climatic index North Atlantic Oscillation Index (NAO) and plume area. More information is given in the text.

Variables	**Precipitation**		**Discharge**		**NAO**		**Plume area**		**PAR**	
	r	*p*	*r*	*p*	*r*	*p*	*r*	*p*	*r*	*p*
Mode 1 *nLw555*-8-day	0.47	< 0.001	0.50	< 0.001					-0.59	<0.0001
Mode 1 *nLw555*-monthly	0.46	< 0.001	0.51	< 0.001					-0.62	<0.0001
Mode 2 *nLw555*-8-day	0.36	< 0.02	0.41	< 0.01					-0.18	<0.05
Mode 1 *Chl*-8-day	0.38	< 0.001	0.47	< 0.001	-0.017	< 0.01			0.05	>0.05
Mode 2 *Chl*-8-day							-0.55	< 0.001	0.67	<0.0001
Mode 2 *Chl*-monthly			0.37	< 0.01					0.71	<0.0001
Mode 1 plume area-monthly	0.63	< 0.01	0.42	< 0.01	-0.52	< 0.001				
Mode 1 mean *nLw555*-monthly					-0.41	< 0.001				
Mode 1 mean *Chl*-monthly					-0.017	< 0.01				

fall events do not tend to match well with discharges to the estuary because of the intense regulation by several reservoirs of the Guadalquivir basin. Furthermore, medium sized discharges may occur without intense local rainfall; for example, see late autumn-winter 2006. However, extreme rainfall events were clearly marked by high discharges from the dam (a protection measure) and clearly coincided with very negative values of the NAO index in 2010, 2011 and 2013 (Fig. 9e). Additionally, a high correlation was found between monthly mean plume area and monthly averaged precipitation (r = 0.63, p < 0.01, Table 4) and monthly river discharge (r = 0.42, p < 0.01, Table 4). Hence, *nLw555* first mode seems to represent variability associated with rainfall and the subsequent terrestrial discharges to the Guadalquivir estuary. The second *nLw555* mode, which showed a similar temporal pattern, was also positively correlated with daily precipitation (r = 0.36, p < 0.02) and discharges (r = 0.41, p < 0.01), suggesting it represented the influence of similar factors.

Modal analyses of Chlorophyll

EOF analysis of 8-day composite [*Chl*] images revealed three statistically significant modes, explaining 31%, 11% and 6% of total variance, respectively (48% of total variance, Fig. 6). The first spatial mode was positive throughout the region, with maximum values observed nearshore and decreasing values offshore, as well as to the South of the region (Fig. 7d). High and low [*Chl*] values on the continental shelf were associated with positive and negative [*Chl*] first mode coefficients observed in winter-spring and summer, respectively (Fig. 8d). Maximum positive amplitudes showed inter-annual variations, with the highest values observed in winter 2011 and spring 2013, whereas negative amplitudes were of a similar magnitude throughout the time-series.

Similarly to the second *nLw555* mode, the second [*Chl*] mode could be classified into two different zones (Fig. 7e). The first zone (A_{2C}) with positive spatial coefficients was located along the coastal fringe, from Isla Cristina (to the north) to Cadiz Bay (to the south), and coincided with the maximum [*Chl*] observed in the monthly composites (Fig. 3b). The second zone (A_{2N}) was located further offshore, extending from the North to the Guadalquivir estuary. This zone was characterized by a negative spatial coefficient, suggesting that negative temporal amplitudes represented higher [*Chl*] values, which are associated with the autumn phytoplankton bloom, as observed in the monthly composites (Fig. 5). Coefficients located further offshore (values ~ 0) suggested relative stability in [*Chl*]. [*Chl*] second mode temporal amplitudes showed a marked seasonality; with positive values during spring-summer and negative during the rest of the year (Fig. 8e). As for *nLw555* second mode, inter-annual variation in the magnitude of negative values was observed, whereas positive peaks were rather constant.

The spatial distribution of [*Chl*] third mode also differentiated two zones (Fig. 7f): The first (A_{3S}) corresponded to a wide area from the Guadalquivir mouth to the South, with positive coefficients. The second (A_{3N}), with negative coefficients, was a narrow band along the coast located further North, centred on the mouths of Tinto-Odiel rivers. Offshore waters again suggested relatively stable [*Chl*] compared to the rest of the region. Examination of the temporal amplitudes of this mode (Fig. 8f) suggested an irregular pattern compared with the other modes and large inter-annual variations.

Comparison of the time-series of [*Chl*] first mode amplitudes with daily rainfall (mm), discharges from the Alcala del Rio dam and the NAO index (Fig. 9, Table 4), revealed that positive amplitudes, generally observed in late autumn, winter and early spring, tended to be associated with periods of high rainfall (r = 0.38, p < 0.001), river discharges (r = 0.47, p < 0.001) and, weakly, with negative NAO values (r = -0.017, p < 0.01). The temporal amplitude confirmed that the seasonal timing of [*Chl*] blooms was consistent between years. Nevertheless, important regional inter-annual variability in bloom size was noted, which was related with the magnitude of these storms. Maximum signals of precipitation were linked to high [*Chl*], as can be observed for example in the most recurrent phytoplankton bloom that occurred during winter 2011-2012 and spring 2013.

Regarding the second [*Chl*] mode, amplitudes were also positively correlated with discharges (r = 0.37, p < 0.01), suggesting that river outflow and high [*TSS*] played a role in controlling bloom dynamics in zone A_{2C}, but not A_{2N}. This was illustrated by examining the plume extent in A_{2C} and the variability in [*Chl*] second mode (Fig. 10). During winter periods, an increase in the extent of the plume occurred in parallel with a decrease in [*Chl*] leading to a negative association between [*Chl*] second mode and plume extent (r = -0.55, p < 0.001, Table 4). Regarding this significant pattern, it appears that secondary bloom episodes with less intense [*Chl*] records took place over the course of the study period. This temporal mode was representative of the semi-annual signal and was coupled with the first mode, presenting a 3-month phase lag supported by the high correlation coefficient between both time series (r = 0.79 , p < 0.001).

Further indications of the role of [*TSS*] in the control of phytoplankton dynamics in the zone directly in front of the estuary mouth can be observed by examining physical-optical parameters at 2 representative sites (Fig.11), the nearshore station 14, and the offshore station 17 (Fig. 1). Mixed layer depth (MLD, in situ data from May 2005 to August 2007 and via the GODAS model from January 2003 to June 2013) showed annual oscillations that were clearly visible at the offshore station (Fig. 11a). This consisted in a deepening of the mixed layer around winter-early spring (25 m-bottom depth and 180 m, for station 14 and 17, respectively) due to convective mixing caused by the winter cooling. MLD became shallower towards the end of spring

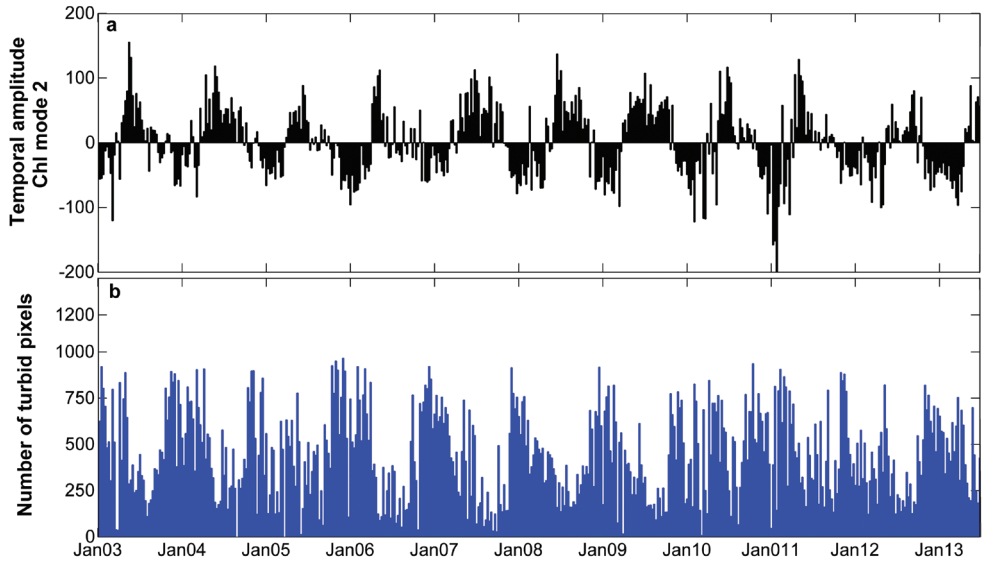

Fig. 10: a) Temporal amplitude of chlorophyll EOF for mode 2, and b) Total number of turbid pixels (*nLw555* values > 1.3 mW/cm^2 µm sr) in the coastal region A_{2C}.

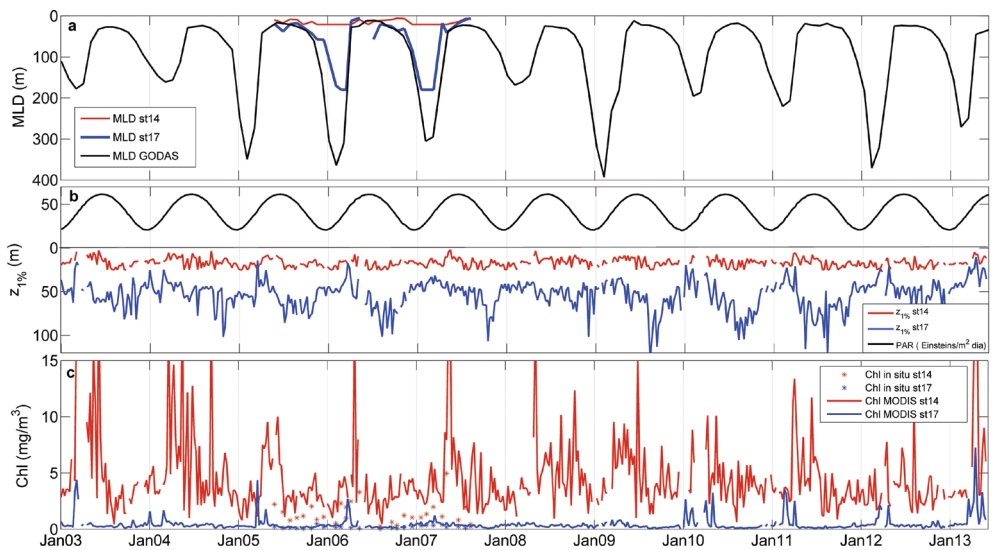

Fig. 11: a) Mixed Layer Depth (MLD, m) from in situ data in the coastal station 14 (red line) and offshore station 17 (blue line) and from the GODAS model in the 2ºx0.6º box (black line), b) Euphotic zone ($z_{1\%}$, m) for both station 14 (red line) and station 17 (blue line), and mean Photosynthetically-Active Radiation (PAR, Einstein / m^2 / day) from MODIS data in the ROI, c) *Chl* concentration (mg/m^3) from in situ data in station 14 (red stars) and 17 (blue stars) and from MODIS corresponding pixel for station 14 (red line) and 17 (blue line).

and into summer (6 m and 5 m for station 14 and 17, respectively) due to warmer waters that systematically emerged in the region (Vargas *et al.,* 2003; Navarro & Ruiz, 2006). The same seasonal evolution was observed in the GODAS model results (average of a 2º x 0.3º box), which also suggested large inter-annual variability. The correlation between in situ MLD and [*Chl*] was $r = 0.21$ (station 14, $p < 0.05$) and $r = 0.55$ (station 17, $p < 0.005$), whereas correlation with modelled MDL corresponded to $r = -0.0018$ (station 14, $p > 0.05$) and $r = 0.44$ (station 17, $p < 0.0001$). In addition, the relationship with [*Chl*] modes was examined resulting in r values of 0.32 ($p < 0.0001$), -0.47 ($p < 0.0001$) and 0.07 ($p < 0.4$) for modes 1, 2 and 3, respectively. On the other hand, $z_{1\%}$ (Fig. 11b) had maximum values in summer and early autumn (25 m-bottom depth and 129 m, station 14 and 17 respectively) and minimum values towards the end of winter and early spring (2.0 m and 10.4 m). This was equivalent to K_d *(PAR)* values of 0.09 and 0.01 m^{-1} at stations 14 and 17, respectively in summer, and 5.65 and 5.67 m^{-1} in winter. Considering that seasonal variations in daily total PAR ranged from 62 to 20 mol photons/m^2/day in summer and winter, respectively (Fig.11b), the high attenuation at station 14 observed in winter appeared to reduce light availability enough to limit phytoplankton productivity, and thus influence [*Chl*] dynamics (Fig. 11c). Indeed, [*Chl*] at station 14 and 17 were not correlated with daily total PAR ($r =$

0.07 and 0.03 for station 14 and 17, respectively; $p > 0.5$), whereas they were correlated with $z_{1\%}$ (r = -0.85 and -0.57 for station 14 and 17, respectively; $p < 0.001$, $n = 498$).

Discussion

Ocean Colour Validation

The exponential relationship between [*TSS*] and the backscattering characteristics of surface waters derived in this study suggests good predictive capacity. Although it must be noted that the relationship is specific for this region and may diverge from other water masses as a consequence of the optical properties of the *TSS*, such as particle types, size, density and composition, as well as due to the *TSS* ranges considered. Comparisons of at-sensor products against field *TSS* or turbidity in coastal areas can be found in the literature (Hu *et al.,* 2004; Otero & Siegel, 2004; Chen *et al*., 2007). There is no agreement about the best class of model to be used. Some suggest it should be logarithmic (e.g. Tassan & Sturm, 1986), log-linear (Chen *et al.,* 1991), linear (Ritchie *et al.,* 1987; Forget & Ouillon, 1998) or exponential (Schiebe *et al.,* 1992; Li & Li, 2000; Hu *et al.,* 2004; Caballero *et al.*, 2014), as used in this study.

A systematic overestimation of MODIS derived [*Chl*] was found in nearshore samples that was not present in the offshore samples. This has been previously observed in other coastal turbid waters (often with large *bias*); indeed the OC3M algorithm (O'Reilly *et al.,* 2000) typically describes 87% of the variance in traditional absorption dominated ocean waters and only 61% in the case of coastal waters. This can be explained by the interference with other absorbing substances such as yellow substance and coloured sediments or detritus (Darecki & Stramski, 2004; Zhang *et al.,* 2006; Werdell *et al.,* 2009). Previous validation exercises conducted by Navarro & Ruiz (2006) between in situ [*Chl*] measurements at 10 m and SeaWiFS data (2000-2002) in the offshore region of Guadalquivir estuary exhibited good correlation (r = 0.85, $p < 0.001$, n = 304). This relationship indicated less overestimation compared to the results of the nearshore stations in this study, but similar to the offshore stations. These issues, combined with failure to correct for atmospheric and land adjacency effects, help explain the higher uncertainty in retrieving coastal [*Chl*]. Several remote sensing derived-[*Chl*] validation studies in coastal domains exhibit similar results (Ruddick *et al.,* 2000; Toole & Siegel, 2001; Otero & Siegel, 2004); predictive uncertainty in coastal waters is generally higher than in the open ocean. Nevertheless, in terms of cost-effective water quality monitoring, ocean colour algorithms from MODIS provided realistic and high-resolution temporal dynamics of [*TSS*] and [*Chl*]. More importantly, these relationships seem to be stable over 2003 and 2007, reinforcing the hypothesis that the regressions are time-independent and the MODIS-derived values are reasonable estimates. The sampling stations were distributed across the coastal region and throughout four seasons, thus representing an overall consistent relationship over the wide range of concentrations measured offshore and within the plume.

Spatio-temporal variability and driving mechanisms

High *nLw555* values occurred near the coast with the largest values principally found near the Guadalquivir river mouth and Cadiz bay in winter (recurrent presence of sediment plumes), presumably mainly due to sediment-laden terrestrial runoff. Across-coast dispersal distances of 50 to 75 km have been reported for the Guadalquivir estuary plume (Navarro *et al.,* 2012b), which seem to be confirmed by this study. The area south of Guadalquivir, Cadiz bay is also influenced by the Guadalete river and fringing wetlands. Contrary to expectations, relatively low *nLw555* values were found in the vicinity of the other two major rivers located in the north of the region (Tinto-Odiel and Guadiana rivers). Suspended materials released from them are presumably rapidly transported to the southeast, the main prevailing ocean circulation in this region (Criado Aldeanueva *et al.,* 2006; García-Lafuente *et al.,* 2006). Hence, this study supports the previous suggestions that the Guadalquivir is the main source of Holocene sediments (Lobo *et al.,* 2004) and probably, dissolved organic material and nutrients (Ribas-Ribas *et al.,* 2011) to the E. Gulf of Cadiz.

EOF analysis revealed the spatio-temporal structure of the river plume and suggested a close connection between *nLw555* dynamics and meteorological conditions. The *nLw555* first mode appeared to be explained by a combination of rainstorm events and river discharge (Díez-Minguito *et al.,* 2012; Navarro *et al.,* 2011, 2012b; Caballero *et al.,* 2014), both strongly correlated with the NAO index. This index, which also correlates with prevailing winds, has previously been show to be an important indicator of the inter-annual variability in the Gulf of Cadiz (Prieto *et al.,* 2009). The second *nLw555* mode generally showed similar temporal variability to the first mode and was also positively correlated with rainfall and discharges from the Guadalquivir. However, this mode had a more localized distribution of positive values in the vicinity of the estuary mouth and a zone with negative values to the north. The coincidence of the second mode high negative values in winter with the positive values of the first mode (e.g. 2010) suggests the influence of shorter time scale events. A possible candidate could be the influence of onshore westerly winds on local circulation. In this line of thinking, third mode seemed to indicate higher [*TSS*] offshore, particularly in front of Cadiz bay, which may suggest the influence of periods with easterly winds blowing offshore.

The link between river plumes and a large terrestrial runoff event is a regular feature of turbid coastal regions (Otero & Siegel, 2004; Nezlin & DiGiacomo, 2005; Thomas & Weatherbee, 2006; Schroeder *et al.,* 2012). At a significant rain event scale, floods create local modifica-

tions of the hydrodynamic conditions in the estuary and, consequently, re-suspension, local erosion of bed and margins, and the deposition of new sediments, influencing coastal waters. Maximum outflow events due to runoff caused high and persistent turbidity peaks in the region (e.g. winter 2010). These episodes have important consequences for the neighbouring coastal zone, which, in turn, can probably be related to elevated concentrations of nutrients, pollutants, etc. In addition, high levels of suspended solids endanger the already fragile balance of an ecosystem subjected to the pressure of apparent human intervention in the area, hindering the operation of aquaculture facilities and the irrigation of numerous cultivated areas in the estuary (Bhat & Blomquist, 2004; Navarro *et al.,* 2012b). In the E. Gulf of Cadiz, which is dominated by the Guadalquivir estuary, [*TSS]* dynamics appear to be a consequence of the superposition of the seasonal variability of rainfall, the irregular discharges from the Alcala del Rio dam, and to a much lesser extent of the prevailing winds.

Multi-year monthly composites of [*Chl*] showed significant seasonal variability in the region, with the highest values observed in early spring and the lowest in late summer. Similar seasonality was also shown by Navarro (2004) using monthly time series for the entire Gulf of Cadiz. The particularity of this study, is the strip with high [*Chl*] observed along the coast in all composites. This could be an artifact of the higher *bias* found in nearshore waters, as discussed above. On the other hand, the highest [*Chl*] values were observed in the nearshore regions influenced by rivers Guadiana, Tinto-Odiel, Guadalquivir and Guadalete. South of Cadiz bay, the nearshore strip was reduced in intensity and width, suggesting that the observed phenomenon is at least in part related to the fertilizing activity of these major riverine inputs, which promote phytoplankton growth. Indeed, previous studies suggest that these rivers, and in particular the Guadalquivir, constitute the major factor determining the primary productivity and fisheries resources of the region (Prieto *et al*., 2009; Ruiz *et al.,* 2009).

The [*Chl*] first mode appeared to capture this seasonal variability with changes in winter-spring phytoplankton blooms throughout the region (extending out onto the continental shelf), and particularly north of the estuary. This typical seasonality is common to many coastal regions (Peliz & Fiúza, 1999; Thomas *et al.,* 2001; Xu *et al.,* 2011; Le *et al.,* 2013), where nutrient-limitation keeps [*Chl*] low in surface waters during summer. As vertical water structure breaks down in autumn-winter and nutrients become available again, phytoplankton blooms are formed, especially in spring as light availability increases. The correlation of [*Chl*] first mode with precipitation and discharges, suggests that inputs of nutrients from the major rivers, fertilizing the surrounding waters (Peliz & Fiúza, 1999; Navarro & Ruiz, 2006; Navarro *et al.,* 2011), modulate this general pattern. These high-flow events have important consequences for the neighbouring coastal zone, pumping large quantities of nutrients and stimulating the growth of phytoplankton that sustains the food chain (Prieto *et al.,* 2009). In addition, the [*Chl*] trend corresponded to a decline until 2009 and, from then onwards, an increase that is indicative of nutrient enrichment in the region during recent years. These phenomena are also associated with a precipitation increment due to frequent storm events and consequent river discharge intensification, as has also been observed in the north-eastern Gulf of Cadiz (Prieto *et al.,* 2009; Navarro *et al.,* 2011).

Second mode appeared to distinguish [*Chl*] dynamics between the narrow nearshore strip directly influenced by the rivers (A_{2C}) and the coastal region to the North (A_{2N}). The latter region coincides with the "Huelva Front" (Stevenson, 1977), which is generated by local upwelling as currents flow over the Cape Santa Maria canyon (increasing nutrient supply to surface waters). The increased tendency for an early breakdown of vertical stratification may account for the late summer-autumn phytoplankton blooms predominantly observed in this zone. The EOF analysis of [*Chl*] conducted in the Gulf of Cadiz by Navarro & Ruiz (2006) exhibited the presence of several zones in second mode. In fact, areas A_{2N} and A_{2C}, differentiated by the second mode in the present study, are closely related to Zone 3 and Zone 4 of their study, respectively.

The particularly high [*Chl*] values in the nearshore strip (A_{2C}) were associated with late spring-summer maximum in the second mode, with a time lag of about a month after peaks in the first mode. This suggests that another factor, such as light, rather than nutrients was limiting primary production in this zone (Eppley & Peterson, 1979). Indeed, studies have shown that the Guadalquivir estuary, which has relatively low [*Chl*], despite extremely high nutrient concentrations, is generally severely light-limited due to very high turbidity levels (Navarro *et al.,* 2012a; Ruiz *et al.* 2006; 2013). This is a common feature of other nutrient-replete, highly turbid estuaries (Wofsy, 1983; Cloern, 1987; Irigoien & Castel, 1997). Evidence that this phenomenon extends into the surrounding coastal zone is provided by in situ vertically resolved data on the physical-optical properties of the water column. Maximum [*Chl*] values were observed earlier at the offshore station (around February) compared to the nearshore station located in the estuary mouth (March-April). During this period, MLD at both stations suggests that water column stratification was not significant; however, higher $K_d(PAR)$ levels, resulting in a shallower $z_{1\%}$ were observed at the nearshore compared to the offshore station. This suggests that light limitation due to high [*TSS*] delays the development of the nearshore spring phytoplankton bloom. At both stations, during the stratification period (summer and early autumn), a seasonal thermocline develops, MLD gets shallower, terrestrial inputs decline and nutrient transport to surface waters is restricted (Sarmiento *et al.,* 1998), leading to lower [*Chl*]. The correlation

between both in situ and modelled MLD and [*Chl*] indicates a more significant cause-effect connection of MLD-bloom patterns at the offshore station than at the nearshore station. The simultaneous coincidence between MLD and [*Chl*] maximum suggests that [*Chl*] peaks after the maximum MLD is formed extending below the euphotic zone, confirming the connection established by Navarro *et al.* (2012a). Hence, the relationship existing between both MLD-$z_{1\%}$ depths and upwelling (Fiúza, 1983; Criado-Aldeanueva *et al.,* 2006) and estuarine processes may explain the detected blooms. Finally, [*Chl*] third mode may suggest the influence of strong easterly winds, particularly dominant in the region during summer, which break-down thermal stratification and transport coastal phytoplankton offshore.

Although the Guadalquivir estuary is typically vertically homogeneous (Vanney, 1970), the occurrence of high-flow events could be responsible for strong vertical stratification. Stratification within the plume can trap biomass in distinct layers where light levels can change in just a meter. The influence of the buoyancy plume could diminish the MLD, hence the mean light intensity entering the MLD increases. As stated above, the outstanding effect of light-limitation in turbid environments illustrates the critical significance of mixing properties within buoyant coastal plumes, as it regulates the potential for productivity. In addition, many factors clearly contribute to [*Chl*] degradation, but phytoplankton decay and predator consumption (grazing) are the main sources of phytoplankton mortality in the oceans; zooplankton was found to respond quickly to variations in phytoplankton biomass (Calbet & Landry, 2004). In that sense, the central role of grazing on phytoplankton population dynamics has been recognized in the Gulf of Cadiz (García *et al.,* 2002).

EOF analysis explained 72% and 50% of the variability in *nLw555* and [*Chl*] respectively, suggesting that particularly for [*Chl*], variation at smaller-scales is probably a key feature. Processes not considered here such as tidal dynamics and grazing (García *et al.,* 2002) may help to further explain this variability. Nevertheless, inter-annual and seasonal patterns in [*TSS*] and [*Chl*] appear to be tightly related to terrestrial discharges, particularly from the Guadalquivir estuary, and to the seasonal interaction between water column stratification and light availability. This sustains the significant relevance of the physical conditions and local processes for the biological response in the region. However, in support of future local pollution assessment activities and decision-making needs, higher resolution ocean colour imagery in both time (e.g. sub-diurnal) and space would be required to recognize and predict events adequately. These emerging capabilities would comprehensively sort out and characterize the small-scale variability of the water properties observed in this coastal region. In this regard, the use of airborne sensors or observational platforms will allow regular real-time monitoring and adequate assessment of the ecological impacts of the turbidity plume. Further investigation is necessary to elucidate critical boundaries and the linkages between water quality, turbidity plumes and phytoplankton growth.

Conclusion

This study demonstrates that remote sensing can serve as a tool to estimate [*TSS*] and [*Chl*] in the coastal waters of the Eastern Gulf of Cadiz. Spatio-temporal analyses of both variables permitted the assessment of driving forces and the connection with climate fluctuations. The outcome of EOF analysis suggests that the Guadalquivir river plume is of considerable importance not only because of its effect on nearshore hydrography, but also because of its influence on biological productivity. The seasonal dynamics of total suspended matter are strongly associated with freshwater discharges from the Alcala del Rio dam that follow episodes of heavy precipitation. Furthermore, bloom development in the coastal fringe appears to be delayed by the extended turbidity plumes observed during the rainy season. The combination of variable riverine inputs and mixing processes, with light limitation due to the turbidity plume, creates a dynamic, diverse transition area that may help to explain the very high productivity of the region. Hence, understanding the dynamics of the Guadalquivir river plume is key to managing the coastal resources in the Eastern Gulf of Cadiz.

Acknowledgements

We would like to thank NASA for distributing the MODIS data used in this study and Junta de Andalucia for in situ data. The authors also thank the crews of the R.V. Regina Maris and B.I.O. García del Cid for support during the cruises. IC is supported by a grant of the Junta de Andalucia PhD fellowship program. EPM is supported by a JAE DOCTORES 2010 contract partly funded by the European Union (European Social Fund, ESF2007-2013) and the Spanish Ministry for Economy and Competitiveness. LP is supported by the Ramón y Cajal program of Spanish MINECO. This work was financially supported by the Junta de Andalucia Projects P09-RNM-4853 and PR11-RNM-7722, E.U. MarinERA Project MedEX (CTM2008-04036-E/MAR) and PERSEUS (FP7-287600).

References

Bailey, S., Wang, M., 2001. Satellite Aerosol Optical Thickness Match-up Procedures. *NASA Technical Memorandum*, 2001, 70-72. Greenbelt, MD: NASA Goddard Space Flight Center.

Baldacci, A., Corsini, G., Grasso, R., Manzella, G., Allen, J. *et al*., 2001. A study of the Alboran sea mesoscale system by means of empirical orthogonal function decomposition of satellite data. *Journal of Marine Systems,* 29 (1), 293-311.

Bhat, A., Blomquist, W., 2004. Policy, politics, and water man-

agement in the Guadalquivir River Basin, Spain. *Water Resources Research*, 40 (8), 1-11.

Björnsson, H., Venegas, S.A., 1997. *A Manual for EOF and SVD Analyses of Climate Data*. Department of Atmospheric and Oceanic Sciences and Centre for Climate and Global Change, McGill University, Technical report, No 97 (1), 52 pp.

Brickley, P.J., Thomas, A.C., 2004. Satellite-measured seasonal and inter-annual chlorophyll variability in the NorthEast Pacific and Coastal Gulf of Alaska. *Deep Sea Research Part II: Topical Studies in Oceanography,* 51 (1), 229-245.

Caballero, I., Morris, E.P., Ruiz, J., Navarro, G., 2014. Assessment of suspended solids in the Guadalquivir estuary using new DEIMOS-1 medium spatial resolution imagery. *Remote Sensing of Environment*, 146, 148-158.

Calbet, A., Landry, M.R., 2004. Phytoplankton growth, microzooplankton grazing, and carbon cycling in marine systems. *Limnology and Oceanography*, 49 (1), 51-57.

Chen, Z., Hanson, J.D., Curran, P.J., 1991. The form of the relationship between suspended sediment concentration and spectral reflectance: its implications for the use of Daedalus 1268 data. *International Journal of Remote Sensing*, 12 (1), 215-222.

Chen, Z., Hu, C., Muller-Karger, F., 2007. Monitoring turbidity in Tampa Bay using MODIS/Aqua 250-m imagery. *Remote Sensing of Environment*, 109, 207-220.

Cloern, J.E., 1987. Turbidity as a control on phytoplankton biomass and productivity in estuaries. *Continental Shelf Research,* 7 (11), 1367-1381.

Criado Aldeanueva, F., García Lafuente, J., Vargas, J.M., Del Rio, J., Vázquez, A. *et al*., 2006. Distribution and circulation of the water masses in the Gulf of Cadiz from in situ observations. *Deep Sea Research II,* 53 (11-13), 1144-1159.

Darecki, M., Stramski, D., 2004. An evaluation of MODIS and SeaWiFS bio-optical algorithms in the Baltic Sea. *Remote Sensing of Environment,* 89 (3), 326-350.

Díez-Minguito, M., Baquerizo, A., Ortega-Sánchez, M., Navarro, G., Losada, M., 2012. Tide transformation in the Guadalquivir estuary (SW Spain) and process-based zonation. *Journal of Geophysical Research,* 117, C03019, doi:10.1029/2011JC007344.

Eppley, R.W., Peterson, B., 1979. Particulate organic matter flux and planktonic new production in the deep ocean. *Nature,* 282 (67), 677-680.

Fiúza, A.F.G., 1983. Upwelling patterns off Portugal. p. 85-98. In: *Coastal Upwelling Its Sediment Record*. Suess, E., Thiede, J., Springer US, New York.

Forget, P., Ouillon, S., 1998. Surface suspended matter off the Rhone river mouth from visible satellite imagery. *Oceanologica Acta*, 21 (6), 739-749.

García, C.M., Prieto, L., Vargas, M., Echevarría, .F., García Lafuente, J., *et al*., 2002. Hydrodynamics and spatial distribution of plankton and TEP in the Gulf of Cadiz (SW Iberian Peninsula). *Journal of Plankton Research,* 24 (8), 817-833.

García-Lafuente, J., Delgado, J., Criado-Aldeanueva, F., Bruno, M., del Rio, J. *et al*., 2006. Water mass circulation on the continental shelf of the Gulf of Cadiz. *Deep Sea Research Part II: Topical Studies in Oceanography*, 53 (11-13), 1182-1197.

González-Mazo, E., Forja, J.M., Gómez-Parra, A., 1998. Fate and distribution of linear alkylbenzene sulfonates in the littoral environment. *Environmental science & technology*, 32 (11), 1636-1641.

Granado-Lorencio, C.,1991. The effect of man on the fish fauna of the River Guadalquivir, Spain. *Fisheries research,* 12 (2), 91-100.

Hu, C., Chen, Z., Clayton, T.D., Swarzenski, P., Brock, J.C. *et al*., 2004. Assessment of estuarine water-quality indicators using MODIS medium-resolution bands: Initial results from Tampa Bay, FL. *Remote Sensing of Environment,* 93, 423-441.

Hurrell, J. W., 1995. Decadal trends in the North Atlantic oscillation. *Science,* 269, 676-679.

Irigoien, X., Castel, J., 1997. Light limitation and distribution of chlorophyll pigments in a highly turbid estuary: the Gironde (SW France). *Estuarine, Coastal and Shelf Science,* 44 (4), 507-517.

Jamet, C., Loisel, H., Kuchinke, C.P., Ruddick, K., Zibordi, G. *et al*., 2011. Comparison of three SeaWiFS atmospheric correction algorithms for turbid waters using AERONET-OC measurements. *Remote Sensing of Environment*, 115 (8), 1955-1965.

Kara, A.B., Rochford, P.A., Hurlburt, H.E., 2000. An optimal definition for ocean mixed layer depth. *Journal of Geophysical Research: Oceans*, 105 (C7), 16803-16821.

Kidd, P., Dominguez-Rodriguez, M., Diez, J., Monterroso, C., 2007. Bioavailability and plant accumulation of heavy metals and phosphorus in agricultural soils amended by long-term application of sewage sludge. *Chemosphere,* 66 (8), 1458-1467.

Kirk, J.T.O., 1983. *Light and Photosynthesis in Aquatic Ecosystems*. Cambridge University Press: Cambridge, MA, USA, 401 pp.

Lahet, F., Forget, P., Ouillon, S., 2001. Application of a colour classification method to quantify the constituents of coastal waters from in situ reflectance sampled at satellite sensor wavebands. *International Journal of Remote Sensing,* 22 (5), 909-914.

Le, C., Hu, C., English, D., Cannizzaro, J., Kovach, C., 2013. Climate-driven chlorophyll-a changes in a turbid estuary: Observations from satellites and implications for management. *Remote Sensing of Environment,* 130, 11-24.

Li, Y., & Li, J., 2000. A suspended sediment satellite sensing algorithm based on gradient transiting from water-leaving to satellite-detected reflectance spectrum. *Chinese Science Bulletin*, *45* (10), 925-931.

Lobo, F., Sánchez, R., González, R., Dias, J., Hernández-Molina, F.J., Fernández-Salas, L. *et al*., 2004. Contrasting styles of the Holocene highstand sedimentation and sediment dispersal systems in the Northern shelf of the Gulf of Cadiz. *Continental Shelf Research,* 24 (4), 461-482.

Loisel, H., Bosc, E., Stramski, D., Oubelkheir, K., Deschamps, P.Y., 2001. Seasonal variability of the backscattering coefficient in the Mediterranean Sea based on satellite SeaWiFS imagery. *Geophysical Research Letters,* 28 (22), 4203-4206.

Lorenz, E.N., 1956. *Empirical orthogonal functions and statistical weather prediction*. Sci. Rep. Statist. Forecasting Proj., Department Meteor., MIT, No 1, 49 pp.

Mendiguchía, C., Moreno, C., García-Vargas, M., 2007. Evaluation of natural and anthropogenic influences on the Guadalquivir River (Spain) by dissolved heavy metals and nutrients. *Chemosphere,* 69 (10), 1509-1517.

Miller, R.L., Del Castillo, C.E., McKee, B.A., 2005. *Remote sensing of coastal aquatic environments: Technologies, techniques and applications*. Springer, Vol. 7, 345 pp.

Morel, A., Gentili, B., Chami, M., Ras, J., 2006. Bio-optical

properties of high chlorophyll Case 1 waters and of yellow-substance-dominated Case 2 waters. *Deep Sea Research Part I: Oceanographic Research Papers*, 53 (9), 1439-1459.

Morel, A., Huot, Y., Gentili, B., Werdell, P.J., Hooker, S.B. *et al*., 2007. Examining the consistency of products derived from various ocean color sensors in open ocean (Case 1) waters in the perspective of a multi-sensor approach. *Remote Sensing of Environment*, 111 (1), 69-88.

Morris, A.W., Allen, J.I., Howland, R.J.M., Wood, R.G., 1995. The estuary plume zone: Source or sink for land-derived nutrient discharges? *Estuarine, Coastal and Shelf Science*, 40 (4), 387-402.

Navarro, G., 2004. *Escalas de variabilidad espacio-temporal de procesos pelágicos en el golfo de Cadiz*. MSc Thesis. University of Cadiz, Spain, 224 pp.

Navarro, G., Ruiz, J., 2006. Spatial and temporal variability of phytoplankton in the Gulf of Cadiz through remote sensing images. *Deep Sea Research Part II: Topical Studies in Oceanography,* 53 (11-13), 1241-1260.

Navarro, G., Gutiérrez, F., Díez-Minguito, M., Losada, M., Ruiz, J., 2011. Temporal and spatial variability in the Guadalquivir estuary: a challenge for real-time telemetry. *Ocean Dynamics,* 61 (6), 753-765.

Navarro, G., Caballero, I., Prieto, L., Vázquez, A., Flecha, S. *et al*., 2012a. Seasonal-to-interannual variability of chlorophyll-*a* bloom timing associated with physical forcing in the Gulf of Cadiz. *Advances in Space Research*, 50 (8), 1164-1172.

Navarro, G., Huertas, I.E., Costas, E., Flecha, S., Díez-Minguito *et al*., 2012b. Use of a Real-Time Remote Monitoring Network (RTRM) to Characterize the Guadalquivir Estuary (Spain). *Sensors,* 12 (2), 1398-1421.

Neckel, H., 1984. The solar radiation between 3300 and 12500 Å. *Solar Physics,* 90 (2), 205-258.

Nezlin, N.P., DiGiacomo, P.M., 2005. Satellite ocean color observations of stormwater runoff plumes along the San Pedro Shelf (Southern California) during 1997-2003. *Continental Shelf Research,* 25 (14), 1692-1711.

Nezlin, N.P., DiGiacomo, P.M., Stein, E.D., Ackerman, D., 2005. Stormwater runoff plumes observed by SeaWiFS radiometer in the Southern California Bight. *Remote Sensing of Environment,* 98 (4), 494-510.

North, G.R., Bell, T.L., Cahalan, R.F., Moeng, F.J., 1982. Sampling errors in the estimation of empirical orthogonal functions. *Monthly Weather Review,* 110 (7), 699-706.

O'Reilly, J.E., Maritorena, S., Siegel, D.A., O'Brien, M.C., Toole, D., Mitchell, B.G. *et al*., 2000. Ocean color chlorophyll a algorithms for SeaWiFS, OC2, and OC4: Version 4. *SeaWiFS postlaunch calibration and validation analyses,* 3, 9-23.

Otero, M.P., Siegel, D., 2004. Spatial and temporal characteristics of sediment plumes and phytoplankton blooms in the Santa Barbara Channel. *Deep Sea Research Part II: Topical Studies in Oceanography,* 51 (10), 1129-1149.

Parsons, T.R., Maita, Y., Lalli, C.M., 1984. *A manual of chemical and biological methods for seawater analysis*. Pergamon Press, Oxford, 173 pp.

Peliz, A., Fiúza, A., 1999. Temporal and spatial variability of CZCS-derived phytoplankton pigment concentrations off the Western Iberian Peninsula. *International Journal of Remote Sensing,* 20 (7), 1363-1403.

Pennock, J.R., 1985. Chlorophyll distributions in the Delaware estuary: Regulation by light-limitation. *Estuarine, Coastal and Shelf Science*, 21 (5), 711-725.

Pierson, D.C., Kratzer, S., Strömbeck, N., Håkansson, B., 2008. Relationship between the attenuation of downwelling irradiance at 490 nm with the attenuation of PAR (400 nm–700 nm) in the Baltic Sea. *Remote Sensing of Environment,* 112 (3), 668-680.

Prieto, L., Navarro, G., Rodríguez-Gálvez, S., Huertas, I.E., Naranjo, J. *et al*., 2009. Oceanographic and meteorological forcing of the pelagic ecosystem on the Gulf of Cadiz shelf (SW Iberian Peninsula). *Continental Shelf Research,* 29 (17), 2122-2137.

Reynolds, C.S., 1998. What factors influence the species composition of phytoplankton in lakes of different trophic state. *Hydrobiologia,* 369/370, 11-26.

Ribas-Ribas, M., Gómez-Parra, A., Forja, J.M., 2011. Spatio-temporal variability of the dissolved organic carbon and nitrogen in a coastal area affected by river input: The North Eastern shelf of the Gulf of Cadiz (SW Iberian Peninsula). *Marine Chemistry,* 126 (1), 295-308.

Ritchie, J.C., Cooper, C.M., Yongqing, J., 1987. Using Landsat multispectral scanner data to estimate suspended sediments in Moon Lake, Mississippi. *Remote Sensing of Environment*, 23 (1), 65-81.

Ruddick, K.G., Ovidio, F., Rijkeboer, M., 2000. Atmospheric correction of SeaWiFS imagery for turbid coastal and inland waters. *Applied optics*, 39 (6), 897-912.

Ruiz, J., Garcia-Isarch, E., Huertas, E., Prieto, L., Juárez, A. *et al*., 2006. Meteorological and oceanographic factors influencing *Engraulis encrasicolus* early life stages and catches in the Gulf of Cadiz. *Deep Sea Research Part II: Topical Studies in Oceanography*, 53 (11), 1363-1376.

Ruiz, J., González-Quirós, R., Prieto, L., Navarro, G., 2009. A Bayesian model for anchovy (*Engraulis encrasicolus*): the combined forcing of man and environment. *Fisheries Oceanography,* 18 (1), 62-76.

Ruiz, J., Macías, D., Losada, M.A., Díez-Minguito, M., Prieto, L., 2013. A simple biogeochemical model for estuaries with high sediment loads: Application to the Guadalquivir River (SW Iberia). *Ecological Modelling,* 265,194-206.

Ruiz, J., Polo, M.J., Díez-Minguito, M., Navarro, G., Morris, E.P. *et al*., 2014. The Guadalquivir Estuary: A Hot Spot for Environmental and Human Conflicts, Chapter 8. Springer International Publishing Switzerland, 199-232.

Sá, C., Da Silva, J., Oliveira, P.B., Brotas, V., 2008. Comparison of MERIS (Algal_1 and Algal_2) and MODIS (OC3M) chlorophyll products and validation with HPLC in situ data collected off the Western Iberian Peninsula. Proceedings *of the 2nd MERIS/(A) ATSR User Workshop,* Frascati, Italy, 22-26.

Sánchez-Lamadrid, A., Ruiz, J., García, E., Juárez, A., Jiménez, T. *et al*., 2003. *Estudio de los recursos pesqueros del Golfo de Cadiz*. Consejería de Agricultura y Pesca, Junta de Andalucia, 35 pp.

Sathyendranath, S., 2000. *Remote Sensing of Ocean Colour in Coastal, and Other Optically-Complex, Waters*. Reports of the International Ocean-Colour Coordinating Group, No 3, 140 pp.

Sarmiento, J.L., Hughes, T.M.C., Stouffer, R.J., Manabe, S., 1998. Simulated response of the ocean carbon cycle to anthropogenic climate warming. *Nature*, 393, 245-249.

Schiebe, F.R., Harrington, Jr., J.A., Ritchie, J.C., 1992. Remote sensing of suspended sediments: the Lake Chicot, Arkansas project. *International Journal of Remote Sensing*, 13 (8), 1487-1509.

Schroeder, T., Devlin, M.J., Brando, V.E., Dekker, A.G., Bro-

die, J.E. *et al*., 2012. Inter-annual variability of wet season freshwater plume extent into the Great Barrier Reef lagoon based on satellite coastal ocean colour observations. *Marine Pollution Bulletin,* 65 (4), 210-223.

Stevenson, R.E., 1977. Huelva Front and Malaga, Spain, Eddy Chain as defined by Satellite and Oceanographic Data. *Deutsche Hydrographische Zeitschrift*, 30 (2), 51-53.

Tassan, S., Sturm, B., 1986. All algorithm for the retrieval of sediment content in turbid coastal waters from CZCS data. *International Journal of Remote Sensing*, 7, 643-655.

Thomas, A., Carr, M.E., Strub, P.T., 2001. Chlorophyll variability in Eastern boundary currents. *Geophysical Research Letters,* 28 (18), 3421-3424.

Thomas, A.C., Weatherbee, R.A., 2006. Satellite-measured temporal variability of the Columbia River plume. *Remote Sensing of Environment,* 100 (2), 167-178.

Toole, D.A., Siegel, D.A., 2001. Modes and mechanisms of ocean color variability in the Santa Barbara Channel. *Journal of Geophysical Research: Oceans (1978–2012),* 106 (C11), 26985-27000.

UNESCO, 1994. *Protocols for the Joint Global Ocean Flux Study (JGOFS) Core Measurements. IOC Manuals and Guides*. Paris, UNESCO, 170 pp.

Valente, A.S., da Silva, J.C., 2009. On the observability of the fortnightly cycle of the Tagus estuary turbid plume using MODIS ocean colour images. *Journal of Marine Systems,* 75 (1), 131-137.

Vanney, J., 1970. *Lhidrologie du Bas Guadalquivir*. Publicaciones del Departamento de Geografía Aplicada, CSIC, Madrid, 176 pp.

Vargas, J., García-Lafuente, J., Delgado, J., Criado, F., 2003. Seasonal and wind-induced variability of sea surface temperature patterns in the Gulf of Cadiz. *Journal of Marine Systems,* 38 (3), 205-219.

Werdell, P.J., Bailey, S.W., Franz, B.A., Harding Jr, L.W.*et al*., 2009. Regional and seasonal variability of chlorophyll-a in Chesapeake Bay as observed by SeaWiFS and MODIS-Aqua. *Remote Sensing of Environment,* 113 (6), 1319-1330.

Wofsy, S., 1983. A simple model to predict extinction coefficients and phytoplankton biomass in eutrophic waters. *Limnology and Oceanography*, 28 (6), 1144-1155.

Xu, Y., Chant, R., Gong, D., Castelao, R., Glenn, S. *et al*., 2011. Seasonal variability of chlorophyll a in the Mid-Atlantic Bight. *Continental Shelf Research,* 31 (16), 1640-1650.

Zhang, C., Hu, C., Shang, S., Müller-Karger, F.E., Li, Y. *et al*., 2006. Bridging between SeaWiFS and MODIS for continuity of chlorophyll-*a* concentration assessments off SouthEastern China. *Remote Sensing of Environment.* 102 (3), 250-263.